European Journal of Radiology 82 (2013) 220–226

Contents lists available at SciVerse ScienceDirect

European Journal of Radiology

journal homepage: www.elsevier.com/locate/ejrad

Quantitative hepatic CT perfusion measurement: Comparison of Couinaud's hepatic segments with dual-source 128-slice CT

Xuan Wang, Hua-dan Xue*, Zheng-yu Jin**, Bai-yan Su, Zhuo Li, Hao Sun, Yu Chen, Wei Liu

The Department of Radiology, Peking Union Medical College Hospital, Dongcheng District, Beijing, 100730, People's Republic of China

ARTICLE INFO

Article history:
Received 9 May 2012
Received in revised form 22 August 2012
Accepted 22 September 2012

Keywords:
Computed tomography
Perfusion
Liver
Regional blood flow
Hemodynamics

ABSTRACT

Purpose: To compare the quantitative liver computed tomography perfusion (CTP) differences among eight hepatic segments.

Materials and methods: This retrospective study was based on 72 acquired upper abdomen CTP scans for detecting suspected pancreas tumor. Patients with primary or metastatic liver tumor, any focal liver lesions except simple cyst (<3 cm in diameter), history of liver operation or splenectomy, evidence of liver cirrhosis or invasion of portal vein were excluded. The final analysis included 50 patients (M:F = 21:29, mean age = 43.2 years, 15–76 years). Arterial liver perfusion (ALP), portal-venous perfusion (PVP), total hepatic perfusion (THP = ALP + PVP), and hepatic perfusion index (HPI) of each hepatic segment were calculated and compared by means of one-way analysis of variance (ANOVA) and the Bonferonni correction method.

Results: Compared to hepatic segments 5, 6, 7 and 8, segments 2 and 3 showed a tendency of higher ALPs, lower PVPs, and higher HPIs, most of which were statistically significant ($p < 0.05$). Hepatic segments 1 and 4 had higher mean values of ALP and HPI and lower mean values of PVP than segments 5, 6, 7 and 8 as well, although no significant differences were detected except for ALP and HPI for liver segments 1 and 7 ($p = 0.001$ and 0.035 respectively), and ALP for liver segments 1 and 5 ($p = 0.039$). Higher ALP and HPI were showed in hepatic segment 3 compared to segment 4 ($p = 0.000$ and 0.000 respectively). No significant differences were found for THP among eight segments.

Conclusions: Intra-hepatic perfusion differences exist in normal hepatic parenchyma especially between lateral sector (segments 2 and 3) and right lobe (segments 5, 6, 7 and 8). This might have potential clinical significance in liver-perfusion-related protocol design and result analysis.

1. Introduction

Computed tomographic perfusion (CTP) is a developing technique for quantitatively evaluating tissue blood perfusion. Compared to other imaging techniques, such as magnetic resonance imaging (MRI), positron emission tomography (PET), single-photon emission computed tomography and contrast-enhanced ultrasound, CTP has special advantages for its easy feasibility, relative low cost and high spatial resolution.

In the past two decades, hepatic CTP has been applied for evaluation of both local and diffuse liver diseases, including assessments of the severity of hepatic fibrosis associated with chronic liver disease [1–4], primary hepatic tumor and cancer metastases [5–9]. These diseases may lead to significant changes in hepatic microcirculation, thus quantification of hepatic perfusion can improve the assessment and management of such conditions. Interest is also increasing in the potential of CTP imaging for prediction of tumor response to therapies [10], and evaluation of hepatic perfusion changes after surgical [11,12] or radiological [13,14] interventions. Although the main interest in liver-related perfusion studies is directed toward the evaluation of pathological conditions, whether the perfusion differences exist among hepatic segments in normal population is not fully explored. In previous studies, a hepatic lesion was often compared to adjacent normally appearing liver tissue which may belong to different hepatic segments [5–7,9]. Knowledge of inter-segment difference would be helpful in such situations.

From a functional anatomy's aspect, the liver is divided into right and left lobes by a major fissure in which the middle hepatic vein lies. Each lobe is divided into 2 sectors. The right hepatic vein divides the right lobe into anterior and posterior sectors while the left hepatic vein divides the left lobe into medial and lateral sectors.

* Corresponding author. Tel.: +86 13 146115223; fax: +86 10 69155509.
** Corresponding author. Tel.: +86 10 69155441; fax: +86 10 69155442.
E-mail addresses: bjdanna95@hotmail.com (H.-d. Xue), jin_zhengyu@163.com (Z.-y. Jin).

0720-048X/$ – see front matter © 2012 Elsevier Ireland Ltd. All rights reserved.
http://dx.doi.org/10.1016/j.ejrad.2012.09.015

The sectors are further divided into eight functionally independent segments in the widely used Couinaud system based on a transverse plane through the bifurcation of the main portal vein. Each segment has its own vascular inflow, outflow and biliary drainage. The anterior sector of the right lobe contains superior (8) and inferior (5) segments. The posterior sector of the right lobe has superior (7) and inferior (6) segments. The medial sector of the left lobe is segment 4 (the quadrate lobe in morphological anatomy). The lateral sector of the left lobe contains segments 2 and 3. Segment 1 (the caudate lobe in morphological anatomy) is a separate structure which receives blood flow from both the right- and left-sided vascular branches. In many pathologic conditions affecting hepatic hemodynamics such as liver fibrosis [15] and Budd-Chiari [16] syndrome, atrophy of the right lobe (segments 5–8) and medial sector (segment 4), as well as hypertrophy of the caudate lobe (segment 1) and lateral segment (segments 2 and 3) could be commonly observed. In right-lobe living-donor liver transplantation situation, marked perfusion imbalance between anterior (segments 5 and 8) and posterior (segments 6 and 7) sectors of liver graft after surgery could also be observed [11]. An assessment of inter-segmental variances in normal liver perfusion would help understanding the physiological hemodynamic background, and thus explaining the different morphologic characteristics among hepatic segments.

Previously, it was impossible to perform such studies due to limited craniocaudal scan coverage of CTP. With the state-of-art technique development, the *z*-axis coverage of CTP scanning protocol has significant extended than before, providing the possibility to evaluate wider coverage of liver [8,17]. Yet few studies of hepatic quantification perfusion comparing eight hepatic segments have been published [17]. Thus the purpose of this study was to compare the quantitative liver CTP difference among eight hepatic segments.

2. Materials and methods

2.1. Patients

The study was based on 72 acquired upper abdomen CTP scans for detecting suspected pancreatic islet cell tumor over a period of 8 months (June 2011–January 2012). Patients with primary or metastatic liver tumor, any focal liver lesions except simple cyst (smaller than 3 cm in diameter), history of liver operation or splenectomy, evidence of liver cirrhosis or invasion of portal vein were excluded. The final analysis included 50 patients (21 male, 29 female, median age 43.2 years [15–76 years]). 23 patients had islet cell tumor (17 were histologically diagnosed). The remaining 27 subjects were normal.

This retrospective study was approved by our institutional review board, and the requirement for informed consent of the individual patients was waived.

2.2. CTP protocols

All CT images were acquired using a second-generation dual-source 128-slice CT scanner (Somatom Definition Flash; Siemens Healthcare (SMS), Forchheim, Germany).

All subjects underwent CTP scan were normal hydration and at least 4 h of fasting. CTP was performed 10 min after our standard 3-phase enhanced CT protocol. For the perfusion study, 50 ml of iopromide (Ultravist 370 mg/ml, Bayer Schering Pharma, Berlin, Germany) was injected in an antecubital vein through an 18-G needle at a flow rate of 5 ml/s followed by 20 ml saline solution. After a delay of 6 s, multiple scans within the defined scan range were obtained using the 4D spiral-mode. The scan range was chosen to be 14.8 cm, from the inferior border of pancreas upwards, with the aim to cover as wide range of liver as possible.

Tube potential was 80 kVp, effective tube current was 150 mAs/rot. Detector width was 3.84 cm, number of scans was 25, scan direction was alternating, the table travel time from one end point to the other was 1.5 s, total examination time was 37 s, slice acquisition was 128 mm × 0.6 mm (using the z-flying spot). Gantry rotation time was 0.28 s.

During perfusion scanning, the patients were instructed to breathe as quietly as possible for the entire duration. Images were reconstructed with a slice thickness of 3 mm and an increment of 3 mm, using a medium smooth tissue convolution kernel (B20f). All images were then transferred to an external workstation (Multi-Modality Workplace, Siemens) for further analysis.

2.3. Image analysis

Automated motion correction was applied in necessary cases using a nonrigid deformable registration technique for anatomic alignment of the multiple scans (Syngo Volume Perfusion CT Body, Siemens). The perfusion was calculated using the maximum slope method. Peak vascular enhancement was determined from a region of interest (ROI) within the abdominal aorta at the level of the hepatic hilus and another one within the portal vein. The time of maximum enhancement within an ROI of spleen was used to separate arterial and portal-venous phases of hepatic enhancement. All ROIs were drawn in transverse orientation images. Examples of ROI placements and time-density curves (TDC) are shown in Fig. 1.

The quantitative values mapped into 3-dimensional stacks of color images of arterial liver perfusion (ALP, in ml per minute per 100 ml), portal-venous perfusion (PVP, in ml per minute per 100 ml), and hepatic perfusion index (HPI = ALP/[ALP + PVP], in %) were measured. Total hepatic perfusion (THP = ALP + PVP) was calculated.

In the Couinaud system, the liver is divided into eight functional segments based on hepatic veins and a transverse plane through the bifurcation of the main portal vein. For the quantitative analysis, ROIs in the center of each segment, excluding large vessels or focal liver lesions if these were present, were defined in every patient. The area of ROI was about 2–3 cm^2. Examples of ROI placements are shown in Fig. 2.

2.4. Estimation of radiation dose

The volume computed tomographic dose index (CTDIvol) and dose-length-product (DLP) of CTP scan were recorded from each patient protocol. The effective radiation dose of CTP was calculated applying a method proposed by the European Working Group for Guidelines on Quality Criteria for CT using the DLP and a conversion coefficient for the abdomen (κ = 0.015 mSv/[mGy cm]).

2.5. Statistical analyses

ALPs, PVPs, THPs and HPIs obtained with the eight hepatic segments were compared by means of one-way analysis of variance (ANOVA) and the Bonferonni correction method.

Software packages (SPSS version 17.0 for Microsoft Windows, SPSS; Medcalc, Medcalc Software) were used for the statistical analyses. Quantitative variables were expressed as mean ± SD, and statistical significance was established at a p value of <0.05.

3. Results

The entire liver could be imaged in 24 of 50 (48%) patients. In 21 patients, the most cranial parts of hepatic segments 2, 4, 7 and 8 were not included in the scan range. The entire hepatic segment 2 was missed in 2 patients. The most cranial part of hepatic segments

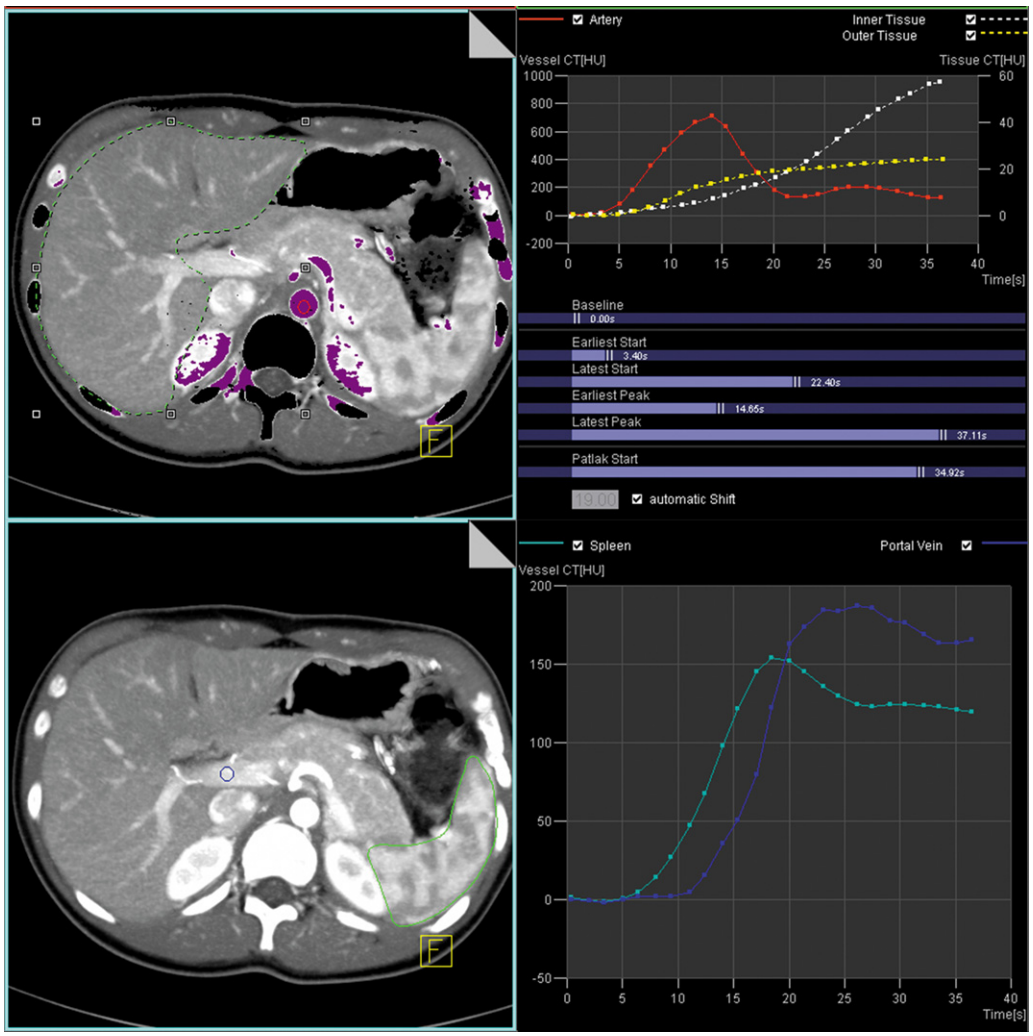

Fig. 1. Definition of the regions of interest (ROI) in the spleen and vessels for quantitative perfusion assessment in a 17-year-old woman with symptoms of hypoglycemia, whose images were normal. Upper left: arterial enhancement was determined by the ROI in the abdominal aorta (red circle) at the level of the hepatic hilum. The dotted green line shows the outlines of the liver volume of interest (VOI). Upper right: the time-density curves (TDCs) of artery, liver VOI (white) and outer tissue (yellow) enhancement. Lower left and right: ROIs and corresponding TDCs for the portal vein (dark blue) and spleen (green or light blue).

7 and 8, and the most caudal part of hepatic segments 5 and 6 were out of scan range in 3 cases as well.

Mean ALPs, PVPs, THPs and HPIs of eight hepatic segments were shown in Table 1. Representative case was shown in Fig. 3.

Compared to hepatic segments 5, 6, 7 and 8, segments 2 and 3 showed a tendency of higher ALPs (comparison of segments 5–8 to segment 2: $p = 0.032$, 0.130, 0.001, 0.009; comparison of segments 5–8 to segment 3: $p = 0.000$, 0.000, 0.000, 0.000), lower PVPs (compared to segment 2, $p = 0.044$, 0.034, 0.286, 0.472; compared to segment 3, $p = 0.004$, 0.003, 0.037, 0.068), and higher HPIs (compared to segment 2, $p = 0.001$, 0.001, 0.000, 0.000; compared to segment 3, $p = 0.000$, 0.000, 0.000, 0.000), most of which were statistically significant. Hepatic segments 1 and 4 had higher mean values of ALP and HPI and lower mean values of PVP than

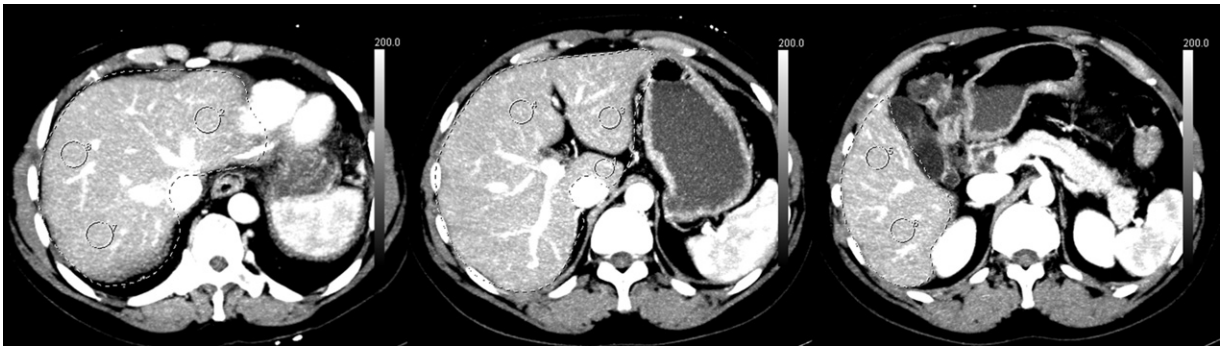

Fig. 2. Images showing the definition of regions of interest (ROI) in eight hepatic segments in the same patient of Fig. 1. Left: ROI of segments 2, 7 and 8. Middle: ROI of segments 1, 3 and 4. Right: ROI of segments 5 and 6.

Table 1
Estimated perfusion values of eight hepatic segments.

Segment	*N*	ALP (ml/min/100 ml)	PVP (ml/min/100 ml)	THP (ml/min/100 ml)	HPI (%)
1	50	11.0 ± 5.5	88.2 ± 25.1	99.2 ± 23.9	12.7 ± 7.2
2	48	11.1 ± 6.3	80.9 ± 28.6	92.0 ± 27.1	14.9 ± 11.5
3	50	13.6 ± 6.6	77.5 ± 24.5	91.1 ± 24.0	17.1 ± 9.5
4	50	9.3 ± 4.1***	88.1 ± 24.6	97.3 ± 24.6	10.4 ± 5.0***
5	50	8.0 ± 3.4*,**,***	98.4 ± 27.4**,***	106.4 ± 27.2	8.7 ± 5.1**,***
6	50	8.4 ± 3.7***	98.8 ± 29.6**,***	107.2 ± 29.1	8.9 ± 4.9**,***
7	50	7.1 ± 3.9*,**,***	95.1 ± 32.6***	102.2 ± 33.1	8.1 ± 6.1*,**,***
8	50	7.6 ± 3.2**,***	94.1 ± 24.6	101.8 ± 24.5	8.6 ± 5.1**,***

* $p < 0.05$ compared with hepatic segment 1.
** $p < 0.05$ compared with hepatic segment 2.
*** $p < 0.05$ compared with hepatic segment 3.

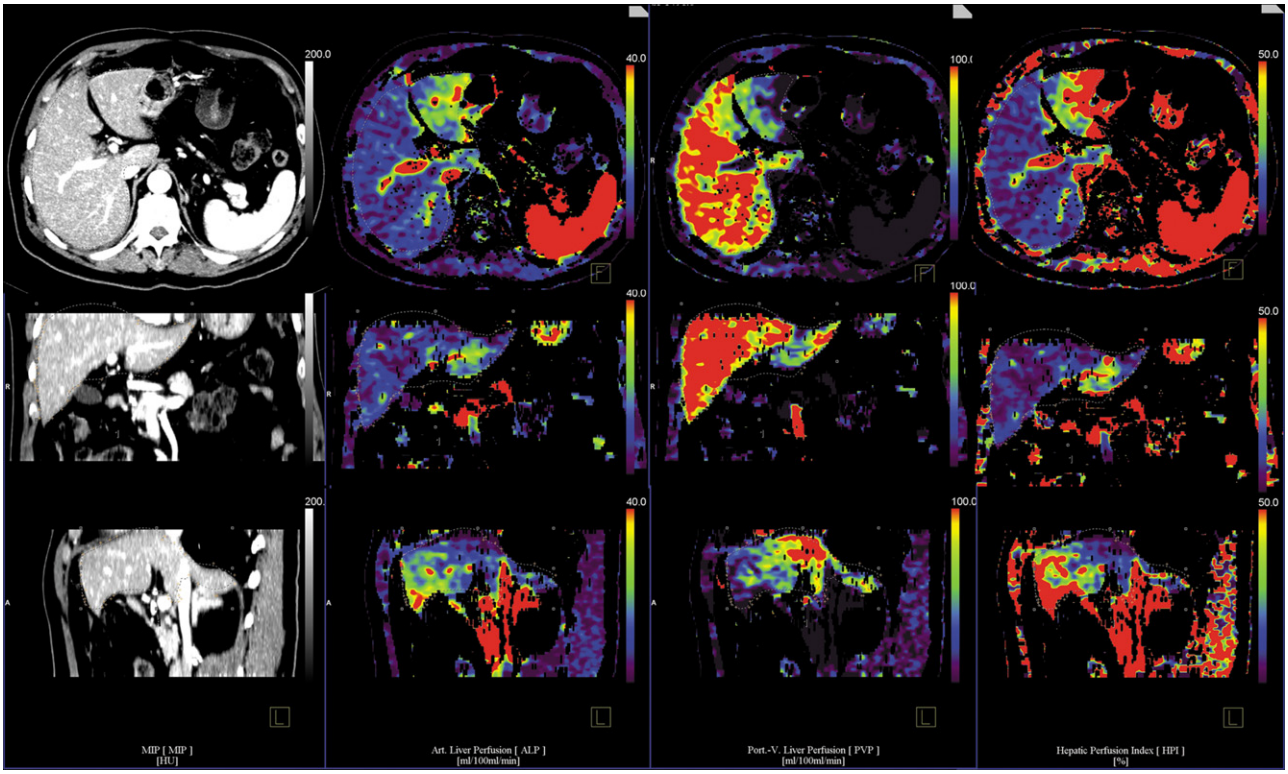

Fig. 3. Images acquired with perfusion CT in a 69-year-old man with histologically diagnosed islet tumor in tail of pancreas. Axial, coronal, and sagittal stacks of the temporal maximum intensity projection (MIP) images and color images of quantitative perfusion parameters including arterial liver perfusion (ALP), portal-venous perfusion (PVP) and hepatic perfusion index (HPI) are shown. Noted the reduced PVP, increased ALP and HPI in the hepatic segments 2 and 3.

segments 5, 6, 7 and 8 as well, although no significant differences were detected except for ALP and HPI for liver segments 1 and 7 ($p = 0.001$ and 0.035 respectively), and ALP for liver segments 1 and 5 ($p = 0.039$). Higher ALP and HPI were showed in hepatic segment 3 compared to segment 4 ($p = 0.000$ and 0.000 respectively). No significant differences were found for THP among eight segments (Table 1 and Fig. 4).

Mean CTDIvol and DLP for CTP were 95.8 ± 0.7 mGy (range: 95.1–96.9) and 1475.0 ± 2.1 mGy cm (range: 1472–1477), respectively. Calculated effective radiation dose for the perfusion scans was 22.1 mSv.

The postprocessing time for one patient was less than 15 min.

4. Discussion

Among various imaging techniques, CTP has special advantages for its easy feasibility and high spatial resolution. However, until recently, multidetector row CT assessment of liver perfusion has been limited by its craniocaudal coverage range. Several techniques from different vendors have been developed to overcome the limitations of the small *z*-axis coverage for CTP imaging, such as a wider detector design [17] or the volume shuttle scan (also called toggling table technique) [8] in which we applied. Such novel technique enables the whole liver perfusion assessment.

Comparing results from different research groups, notable variances could be found in values of each parameter of normal liver parenchyma as follows: ALPs were reported from 12 to 31 ml/min/100 ml, PVPs were ranged from 32 to 132 ml/min/100 ml, and HPIs varied between 12% and 32% [1–4,8,12,18]. The PVPs (77.5–98.8 ml/min/100 ml) in this study were concordant with previous experiments, whereas the ALPs (7.1–13.6 ml/min/100 ml) and HPIs were lower (8.1–17.1%) than those reported in the published data, especially HPIs. Lower value of HPIs mainly resulted from the decrease of ALPs. We hypothesize

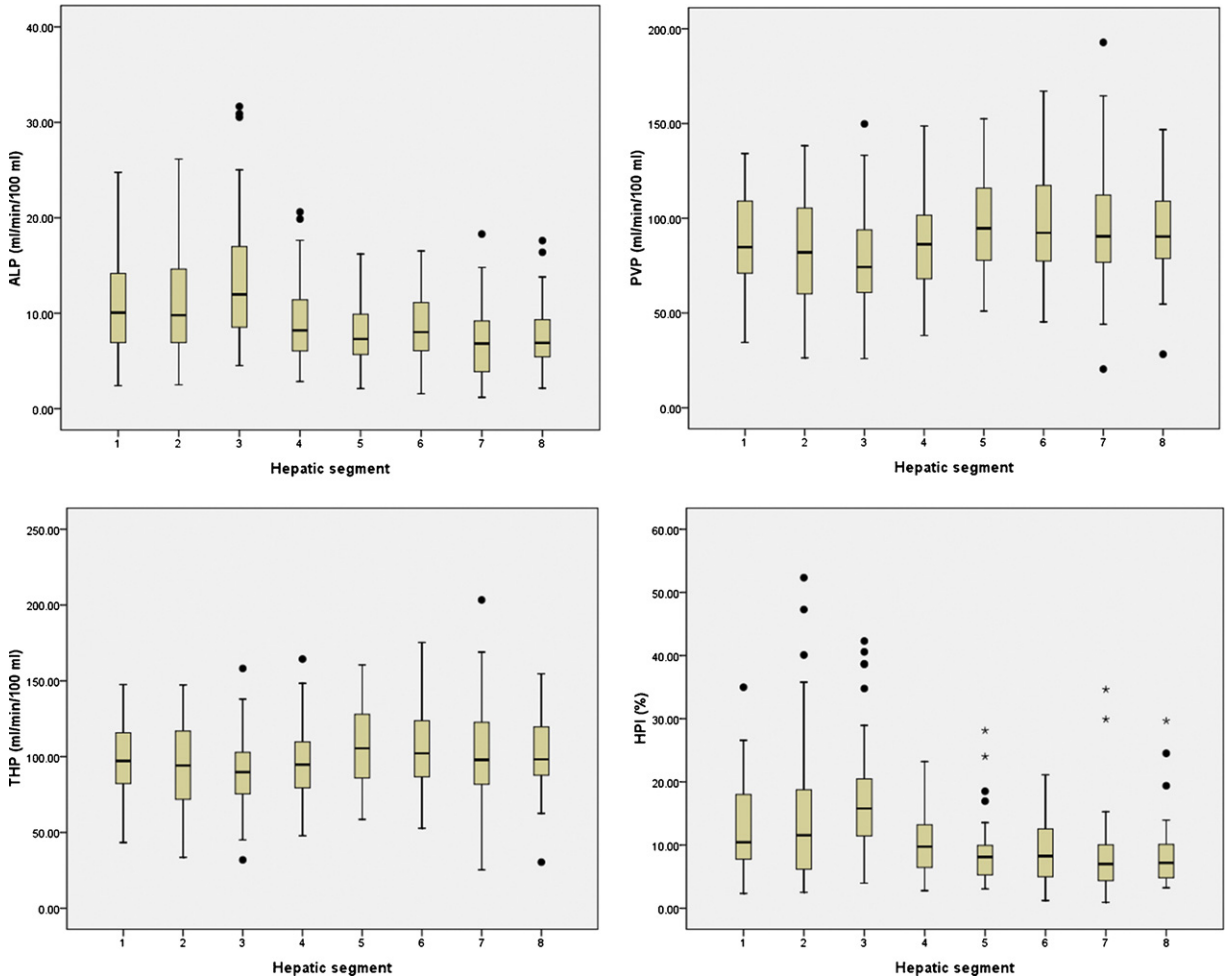

Fig. 4. Box-plots show arterial liver perfusion (ALP), portal-venous perfusion (PVP), total hepatic perfusion (THP) and hepatic perfusion index (HPI) comparisons among eight hepatic segments. ALP and HPI were increased, and PVP were decreased in lateral sector (hepatic segments 2 and 3) compared to right lobe (segments 5, 6, 7 and 8). Box lower and upper boundaries = 25th and 75th percentiles, respectively. Center lines = medians. Error bars = 10th and 90th percentiles.

that the different outcome of ALPs in our study may owe to the different scan and injection protocol, or patients' population bias in age and gender distribution (the objects are relative younger and female dominant in this study) [1,8,12,18]. Physiologically, no recognized human hepatic perfusion values were reported in the literature to the best of our knowledge. Thus, quantitative phantom studies may be required in future to give the reference values and to further interpret these differences as a gold standard.

The result of present study showed that inter-segmental differences do exist in ALP, PVP and HPI. Lateral sector of left lobe (hepatic segments 2 and 3) has higher ALPs, lower PVPs and higher HPIs compared to the others, especially right lobe (segments 5–8). This result is in agreement with that of Barbaro's study: there is a preferential distribution of the portal venous flow to the right lobe of the liver [19]. There are several possible explanations to it. One is anatomic factor. The left branch of portal vein has a smaller caliber [19] and longer course than the right one, and the segments 2 and 3 located in its distal part, resulting in a relatively less portal blood supply to them. The ALPs and HPIs of hepatic segments 2 and 3 are raised for compensation. The second one is position factor. The patient was in supine position during whole scan. The left lobe was in upward location, especially hepatic segments 2 and 3 due to their slender shape, so higher blood pressures were required to maintain same blood inflow comparing to downward location. The pressure of portal vein is much lower than hepatic artery, and the portal vein perfusion to these areas is more likely to be affected. Further investigation is required to confirm this hypothesis.

The result of this study has its related clinical significance. First of all, this result may help explaining the left lobe enlargement in the progression of hepatic fibrosis. Previous studies have showed a decrease in portal venous perfusion and an increase in arterial perfusion in patients with cirrhosis [1–4]. Since the lateral sector of left lobe has higher HPIs, its relative enlargement may be due to artery overflow in cirrhosis condition, and a less important portal flow may also partially protect the parenchyma towards the evolution of cirrhosis. Besides, the awareness of inter-segment difference is important for hepatic CTP researches. In previous studies, a regional hepatic lesion was often compared to adjacent normally appearing hepatic parenchyma which may belong to different hepatic segment [5–7,9], and global changes of diffuse liver diseases were usually described and discussed without precondition of existing inter-segment difference [1–4]. The finding of our study might have potential value in liver-perfusion-related protocol design and result analysis.

To the best of our knowledge, only one study from Kanda's group has been published comparing eight hepatic segments [17]. No significant differences were found in Kanda's study [17] except between HPIs for hepatic segments 3 and 5, which was explained as effects of artifacts. Interestingly, we found similar variances exist in Kanda's result of segments 2 and 3 versus segments 4, 5, 6, 7 and

8. Segments 2 and 3 had higher ALPs, lower PVPs and higher HPIs (ALP: 28.5–29.3 vs. 23.2–25.0, PVP: 95.6–107.3 vs. 114.0–118.7, all in ml/min/100 ml; HPI: 25.0–26.4 vs.18.6–21.0, in %) [17], although without statistically significance. We hypothesize that the different outcome of our study may due to the relative larger study cohort, and a different scan and injection protocol. Besides, we also noticed that in the illustration of normal liver from Miles' study [4], the color scales of HPI and ALP at hepatic hilum level had showed similar difference distribution as our outcomes, but no further comparison was discussed in his study.

In this study, we found that hepatic segments 1 and 4 showed higher ALPs and HPIs and lower PVPs than segments 5, 6, 7 and 8 as well, although most comparisons were without statistical significance. Further study is required with larger amount of patients to prove this possible difference. If the differences do exist, the responsible mechanism for hepatic segment 4 may be similar to hepatic segments 2 and 3 as discussed above. For hepatic segment 1 (the caudate lobe), its portal veins are the proximity veins to the main portal vein and have a shorter intrahepatic course, and its emissary veins pass directly to the inferior vena cava [20]. The complex blood supply and venous drainage of caudate lobe may possibly explain the differences in perfusion parameters compared to other hepatic segments.

For ethical reasons we only included patients with suspicion of pancreatic islet cell tumor to represent the general population in this retrospective study. Strict exclusion criteria were applied to minimize the potential influence of selection bias: subjects with evidence of cirrhosis or invasion of portal vein were not included, and those with focal liver lesion were also excluded except hepatic cysts which were smaller than 3 cm in diameter. Small simple cyst has neither blood supply nor mass effect, so that it can be avoided in ROI drawing. Perfusion parameters including blood volume and permeability were not evaluated in this study because they are based on single input model only. Since our study object was normal liver which has both artery and portal vein supply, a comparison of these parameters would be misleading. These indexes are potentially meaningful and commonly reported in the evaluation of tumor-related angiogenesis and therapy follow-up studies [5–7,9,10].

This study has several limitations. First, our study suffers from a relative limited number of patients, which can limit statistical power, further study with a larger cohort may be necessary. The impact of age and sex to the perfusion parameters were not evaluated therefore. One previous study showed male or younger patients tend to have higher ALP and HPI [18]. Second, compared to the previous studies, the CTDIvol and DLP in our research were increased due to the wide craniocaudal scan range and relative large number of scans [8,17,18]. To date, many techniques have been used to reduce radiation exposure in body CT. The radiation dose can be lowered in the future combining with further optimized perfusion imaging protocols. Third, although the *z*-axis coverage was large, the entire hepatic segment 2 was not included in 2 cases, and the entire liver could only be imaged in 48% patients. It is partially because that the scans were aimed to include entire pancreas as a precondition. In another study of same scan range, the rate that the entire liver could be imaged was higher [8]. However, for cases in which entire liver had not been imaged, the majority of volume has already been covered. Because only the most cranial and/or caudal part of liver were not included in the scan range, which merely accounts for one or two slices in most occasions. Thus this limitation does not significantly impair the effectiveness of our result. Fourth, among several modes including maximum slope, dual-input single compartment, and deconvolution methods, we only applied maximal slope mode to calculate perfusion values. However, due to the relative simple underlying principle, maximal slope mode is the dominate one in the field of liver perfusion measurement and is widely applied in many studies [3–8,10,12–14,17]. Further studies are required to confirm our findings and to better understand segmental variances of hepatic parenchyma, both in normal and pathological conditions.

Despite these limitations, our study has shown that it is feasible to conduct quantitative hepatic perfusion measurements with dual-source 128-slice CT volume shuttle scan, and intrahepatic-segmental perfusion differences exist in normal hepatic parenchyma especially between lateral sector and right lobe. This might have potential clinical significance in liver-perfusion-related protocol design and result analysis.

Conflict of interest

The author certifies that there is no actual or potential conflict of interest in relation to this article.

Acknowledgments

We would thank Dr. Ernst Klotz (Siemens Healthcare, Forchheim, Germany) and Jiu-hong Chen (Medical Solutions, Siemens Ltd., Beijing, People's Republic of China) for their elaborate and warmhearted supports on the final article revision and polishing.

References

[1] Van Beers BE, Leconte I, Materne R, Smith AM, Jamart J, Horsmans Y. Hepatic perfusion parameters in chronic liver disease: dynamic CT measurements correlated with disease severity. American Journal of Roentgenology 2001;176(3):667–73.
[2] Hashimoto K, Murakami T, Dono K, et al. Assessment of the severity of liver disease and fibrotic change: the usefulness of hepatic CT perfusion imaging. Oncology Reports 2006;16(4):677–83.
[3] Nakashige A, Horiguchi J, Tamura A, Asahara T, Shimamoto F, Ito K. Quantitative measurement of hepatic portal perfusion by multidetector row CT with compensation for respiratory misregistration. British Journal of Radiology 2004;77(921):728–34.
[4] Miles KA, Hayball MP, Dixon AK. Functional images of hepatic perfusion obtained with dynamic CT. Radiology 1993;188:405–11.
[5] Ippolito D, Capraro C, Casiraghi A, Cestari C, Sironi S. Quantitative assessment of tumour associated neovascularisation in patients with liver cirrhosis and hepatocellular carcinoma: role of dynamic-CT perfusion imaging. European Radiology 2012;22(4):803–11.
[6] Ippolito D, Sironi S, Pozzi M, et al. Hepatocellular carcinoma in cirrhotic liver disease: functional computed tomography with perfusion imaging in the assessment of tumor vascularization. Academic Radiology 2008;15(7):919–27.
[7] Ippolito D, Sironi S, Pozzi M, et al. Perfusion CT in cirrhotic patients with early stage hepatocellular carcinoma: assessment of tumor-related vascularization. European Journal of Radiology 2010;73(1):148–52.
[8] Goetti R, Leschka S, Desbiolles L, et al. Quantitative computed tomography liver perfusion imaging using dynamic spiral scanning with variable pitch: feasibility and initial results in patients with cancer metastases. Investigative Radiology 2010;45(7):419–26.
[9] Sahani DV, Holalkere NS, Mueller PR, Zhu AX. Advanced hepatocellular carcinoma: CT perfusion of liver and tumor tissue—initial experience. Radiology 2007;243:736–43.
[10] Anzidei M, Napoli A, Zaccagna F, et al. Liver metastases from colorectal cancer treated with conventional and antiangiogenetic chemotherapy: evaluation with liver computed tomography perfusion and magnetic resonance diffusion-weighted imaging. Journal of Computer Assisted Tomography 2011;35(6):690–6.
[11] Qian LJ, Zhuang ZG, Cheng YF, Xia Q, Zhang JJ, Xu JR. Hemodynamic alterations in anterior segment of liver graft after right-lobe living-donor liver transplantation: computed tomography perfusion imaging findings. Abdominal Imaging 2010;35(5):522–7.
[12] Bader TR, Herneth AM, Blaicher W, et al. Hepatic perfusion after liver transplantation: noninvasive measurement with dynamic single-section CT. Radiology 1998;209:129–34.
[13] Meijerink MR, van Waesberghe JH, van der Weide L, et al. Early detection of local RFA site recurrence using total liver volume perfusion CT initial experience. Academic Radiology 2009;16(10):1215–22.
[14] Weidekamm C, Cejna M, Kramer L, Peck-Radosavljevic M, Bader TR. Effects of TIPS on liver perfusion measured by dynamic CT. American Journal of Roentgenology 2005;184(2):505–10.
[15] Shim JH, Yu JS, Chung JJ, Kim JH, Kim KW. Segmental difference of the hepatic fibrosis from chronic viral hepatitis due to hepatitis B versus C virus infection: comparison using dual contrast material-enhanced MRI. Korean Journal of Radiology 2011;12(4):431–8.

[16] Kamath PS. Budd-Chiari syndrome: radiologic findings. Liver Transplantation 2006;12(11 Suppl. 2):S21–2.
[17] Kanda T, Yoshikawa T, Ohno Y, et al. Perfusion measurement of the whole upper abdomen of patients with and without liver diseases: initial experience with 320-detector row CT. European Journal of Radiology 2012;81(11):3048–54.
[18] Kanda T, Yoshikawa T, Ohno Y, et al. CT hepatic perfusion measurement: comparison of three analytic methods. European Journal of Radiology 2012;81(9):2075–9.
[19] Barbaro B, Palazzoni G, Prudenzano R, Cina A, Manfredi R, Marano P. Doppler sonographic assessment of functional response of the right and left portal venous branches to a meal. Journal of Clinical Ultrasound 1999;27(2): 75–80.
[20] Dodds WJ, Erickson SJ, Taylor AJ, Lawson TL, Stewart ET. Caudate lobe of the liver: anatomy, embryology, and pathology. American Journal of Roentgenology 1990;154(1):87–93.